NACA RM A51A09

NACA

RESEARCH MEMORANDUM

PRELIMINARY DATA ON THE EFFECT OF BODY-NOSE BLUNTNESS ON THE DRAG AND PRESSURE RECOVERY OF A SIDE-INLET-BODY COMBINATION AT MACH NUMBERS OF 1.4 AND 1.7

By John F. Stroud and Warren E. Anderson

Ames Aeronautical Laboratory
Moffett Field, Calif.

NATIONAL ADVISORY COMMITTEE
FOR AERONAUTICS

WASHINGTON
April 25, 1951

NATIONAL ADVISORY COMMITTEE FOR AERONAUTICS

RESEARCH MEMORANDUM

PRELIMINARY DATA ON THE EFFECT OF BODY-NOSE BLUNTNESS ON THE DRAG AND PRESSURE RECOVERY OF A SIDE-INLET-BODY COMBINATION AT MACH NUMBERS OF 1.4 AND 1.7

By John F. Stroud and Warren E. Anderson

SUMMARY

The pressure recovery, mass flow, and drag of a twin-scoop, side-inlet-body combination were measured at Mach numbers of 1.4 and 1.7. The inlet was located on a body having an ogival nose followed by a cylindrical section and having a total fineness ratio of 5. Tests were made with this nose and with the nose modified to give various degrees of bluntness. The results indicate that the rounded-nose model with the smallest degree of bluntness tested had only a small detrimental effect on inlet pressure recovery, mass-flow ratio, and drag. The largest degree of nose bluntness, however, caused significant reductions in maximum pressure recovery and mass-flow ratio and a large increase in drag. At a Mach number of 1.7, the largest degree of nose bluntness caused a decrease in maximum pressure recovery of 0.06, a decrease in maximum mass-flow ratio of 0.065, and, for a mass-flow ratio of 0.90, an increase in drag of the body-duct combination of about 135 percent. Generally, similar results were obtained at a Mach number of 1.4.

INTRODUCTION

A program to determine the practicability of side inlets for the air-induction system of present and future high-speed aircraft is in progress at the Ames Aeronautical Laboratory. Information on the overall characteristics of this type of inlet mounted on a sharp-nosed body is presented in reference 1.

From aerodynamic considerations, a slender, pointed nose is desirable for the bodies of high-speed aircraft; however, the operation of equipment to be carried in the nose requires consideration of blunt bodies. In order to assess the aerodynamic penalties involved in the use of a blunt nose shape, an investigation of the effects of body-nose bluntness on the drag, pressure recovery, and mass flow of a twin-scoop, side-inlet-body combination has been made. The preliminary results of this investigation are presented in this report without analysis to expedite publication.

NOTATION

A cross sectional area, square feet

A_{REF} reference area (largest frontal area of model exposed to stream)

a speed of sound, feet per second

C_{D_e} total external drag coefficient

$$\left\{C_{D_e} = -\frac{F_G}{q_o A_{REF}} + \left[\frac{H_o}{q_o}\left(\frac{p_3}{H_o} - \frac{p_o}{H_o} + 2\frac{q_3}{H_3}\frac{H_3}{H_o}\right)\frac{A_3}{A_{REF}} - 2\frac{A_1}{A_{REF}}\frac{m_1}{m_o}\right]\right.$$

$$\left. + \sum\left(P_{BASE}\frac{A_{BASE}}{A_{REF}}\right) - \sum\left(\Delta P_x \frac{\Delta A_{FUSELAGE}}{A_{REF}}\right)\right\}$$

F_G force measured by balance gage, pounds

H total pressure $\left[p\left(1 + \frac{\gamma-1}{2}M^2\right)^{\frac{\gamma}{\gamma-1}}\right]$, pounds per square foot absolute

M Mach number $\left(\frac{V}{a}\right)$, dimensionless

m mass-flow rate (ρVA), slugs per second

p static pressure, pounds per square foot absolute

P static-pressure coefficient $\left(\frac{p-p_o}{q_o}\right)$

q dynamic pressure $\left(\frac{1}{2}\rho V^2\right)$, pounds per square foot

V velocity, feet per second

X_n distance forward on nose from start of constant-cross-section body, inches

X duct station downstream of entrance, inches

r local nose radius, inches

α angle of attack, degrees

γ ratio of specific heats, dimensionless

Subscripts

o free stream

1 inlet station

3 settling chamber

4 exit throat

x station on fuselage

APPARATUS

Wind Tunnel

The investigation was performed in the Ames 8- by 8- inch supersonic wind tunnel at Mach numbers of 1.4 and 1.7. The Reynolds number per foot of length was approximately 8 million at the lowest Mach number and 9 million at the highest. A detailed description of the tunnel and its auxiliary equipment is presented in reference 2.

Model

The four models tested differed only in nose shape; the model dimensions are shown in figure 1. The forebody of the basic model (nose A) consisted of a 10-caliber ogival nose of circular cross section followed by a cylindrical section to the inlet ramp. Nose B was parabolic in longitudinal section and became tangent to the basic nose ogive 0.50 inch from the basic nose tip. Noses C and D were elliptic in shape with the points of tangency to the basic body occurring at the beginning of the cylindrical section. On the basic model (nose A) the twin-scoop inlet was located five body diameters behind the apex of the ogive and enclosed approximately 19 percent of the maximum circumference of the forebody. The inlet area, including both scoops, was 18.2 percent of the total frontal area immediately aft of the inlet station. As shown in figure 1, each scoop was preceded by a 4° ramp. A sharp edge was used on the duct lips with the outer lip surface inclined 3° to the model center line at the upper wall and 5° at the side walls. The

duct passage consisted of a constant area section for a length of two inlet heights aft of the entrance, followed by a subsonic diffuser. The internal cross sectional area variation as a function of distance from the duct entrance is presented in figure 2.

INSTRUMENTATION

Figure 3 shows the support and instrumentation used in this investigation to obtain simultaneous measurements of drag force, mass flow, and pressure recovery. The model was mounted on a steel shell which floated on three rows of bearing balls inside a stationary shell supported by two struts. A shroud provided a fairing between the base of the model and the outer shell. The axial force on the model and inner shell was measured by a strain gage. The pressure of the diffused air within the settling chamber was measured by a survey rake consisting of four total and three static pressure tubes. This rake was arranged so that it could be rotated about the axis of the settling chamber from outside the wind tunnel. The mass flow through the ducts was controlled by an adjustable outlet consisting of a stationary ring and an adjustable plug which was also operated from outside the wind tunnel.

All pressures measured in this investigation were photographically recorded from a multiple-tube mercury manometer. Drag forces acting on the balance strain gage were obtained from deflections of a dynamically balanced galvanometer. Flow about the model was observed and photographed through a schlieren apparatus having a knife edge parallel to the direction of the free stream. Readings of pressure and drag force were taken at 10 angular positions of the survey rake for each mass-flow ratio.

REDUCTION OF DATA

The total pressure ratio H_3/H_0 is a weighted average based on the area surveyed by each rake tube.

The mass-flow ratio, defined as the ratio of mass flowing through the diffuser to that flowing in the free stream through an area equal to that of the entrance, was calculated by the following relation:

$$\frac{m_1}{m_0} = \left(\frac{H_3}{H_0} \right)_{AV} \times \frac{A_4}{A_1} \times \frac{1}{M_0} \left(\frac{2}{\gamma+1} + \frac{\gamma-1}{\gamma+1} M_0^2 \right)^{\frac{\gamma+1}{2(\gamma-1)}} \times K$$

The correction factor K was necessary because the original assumption of sonic velocity throughout the outlet area controlled by the ring and plug (see fig. 3) was not valid near the maximum mass-flow ratio. In this range, a calibration showed the average correction factor to be from 88 to 92 percent of the indicated mass-flow ratio.

The external drag force of the body-inlet combination is defined as the difference between the corrected measured drag force and the momentum change from the free stream to the rake survey station of the mass of air that flowed through the inlet. The data were corrected to account for the fact that the pressure at the base of the model was not equal to the free-stream static pressure. The measured drag force was also corrected for buoyancy forces resulting from the static pressure gradient in the wind tunnel.

RESULTS

The variations of total pressure ratio and external drag coefficient with mass-flow ratio for the four nose shapes are presented in figure 4. The data obtained at a Mach number of 1.4 are shown in figure 4(a) and those obtained at a Mach number of 1.7 are shown in figure 4(b). Schlieren photographs of the model with noses A and D at the two test Mach numbers and maximum mass-flow ratios are shown in figure 5.

It is apparent that the change from nose A to nose B had small effect. However, the change from nose A to nose D caused a decrease in maximum pressure recovery of 0.06, a decrease in maximum mass-flow ratio of 0.065, and, for a mass-flow ratio of 0.90, an increase in drag of the body-duct combination of about 135 percent at a Mach number of 1.7. Generally, similar results were obtained at a Mach number of 1.4.

Ames Aeronautical Laboratory,
National Advisory Committee for Aeronautics,
Moffett Field, Calif.

REFERENCES

1. Davis, Wallace F., Edwards, Sherman S., and Brajnikoff, George B.: Experimental Investigation at Supersonic Speeds of Twin-Scoop Duct Inlets of Equal Area. IV - Some Effects of Internal Duct Shape Upon an Inlet Enclosing 37.2 Percent of the Forebody Circumference. NACA RM A9A31, 1949.

2. Davis, Wallace F., Brajnikoff, George B., Goldstein, David L., and Spiegel, Joseph M.: An Experimental Investigation at Supersonic Speeds of Annular Duct Inlets Situated in a Region of Appreciable Boundary Layer. NACA RM A7G15, 1947.

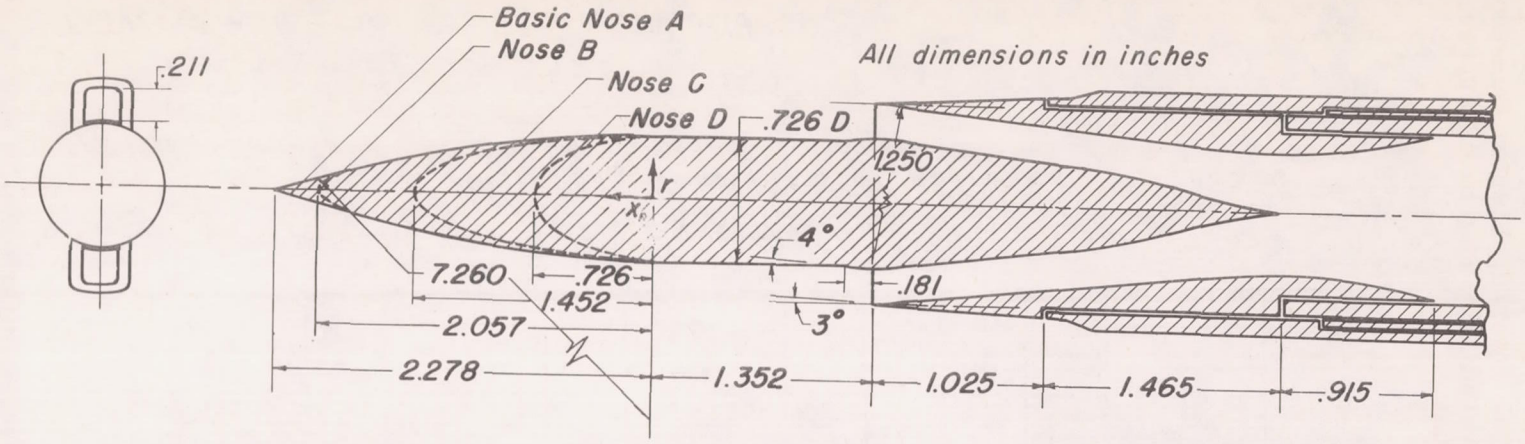

Nose B	
x_n	r
1.778	0.141
1.817	0.131
1.857	0.119
1.882	0.112
1.907	0.103
1.932	0.094
1.957	0.084
1.987	0.071
2.002	0.063
2.017	0.053
2.032	0.042
2.042	0.033
2.057	0

Nose C	
x_n	r
0	0.363
0.250	0.358
0.500	0.341
0.750	0.311
1.000	0.263
1.100	0.237
1.200	0.204
1.300	0.162
1.350	0.134
1.375	0.117
1.400	0.096
1.415	0.081
1.425	0.070
1.435	0.055
1.452	0

Nose D	
x_n	r
0	0.363
0.100	0.360
0.200	0.349
0.300	0.330
0.400	0.303
0.450	0.285
0.500	0.263
0.550	0.237
0.600	0.204
0.650	0.162
0.675	0.134
0.685	0.120
0.700	0.096
0.710	0.076
0.726	0

NACA

Figure 1.– Model dimensions.

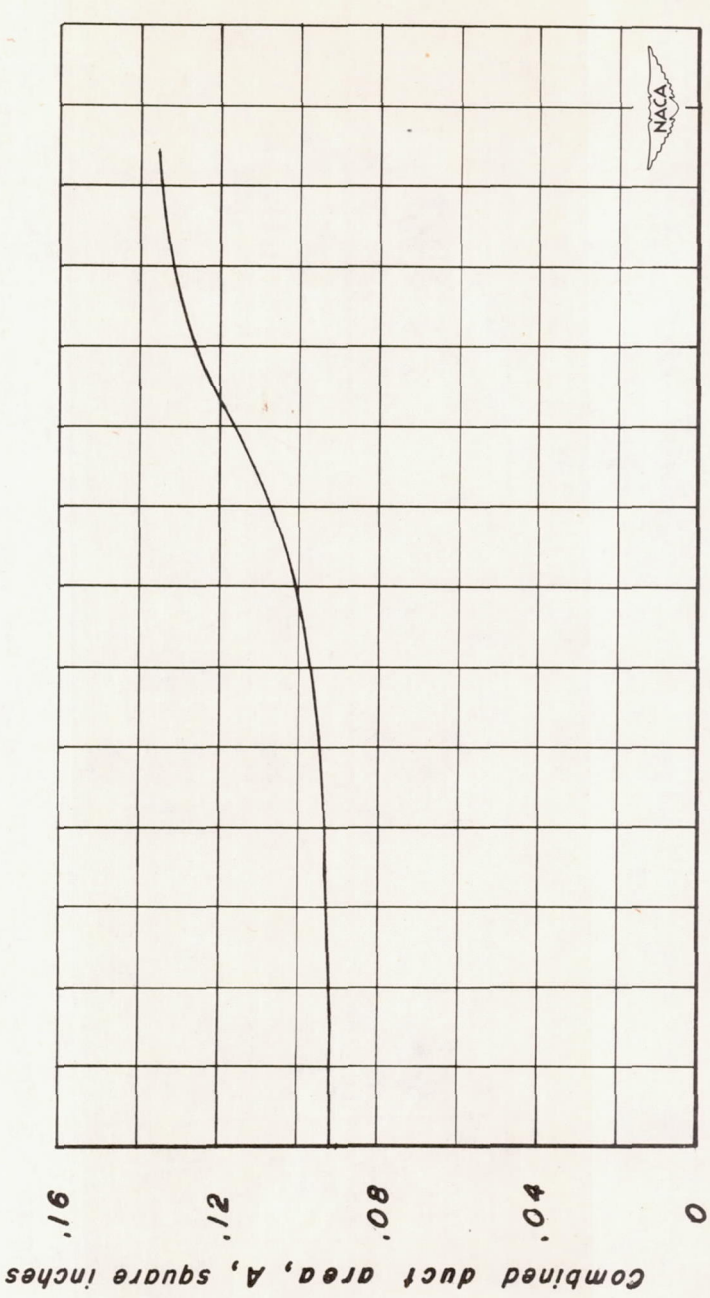

Figure 2.- Internal duct area variation.

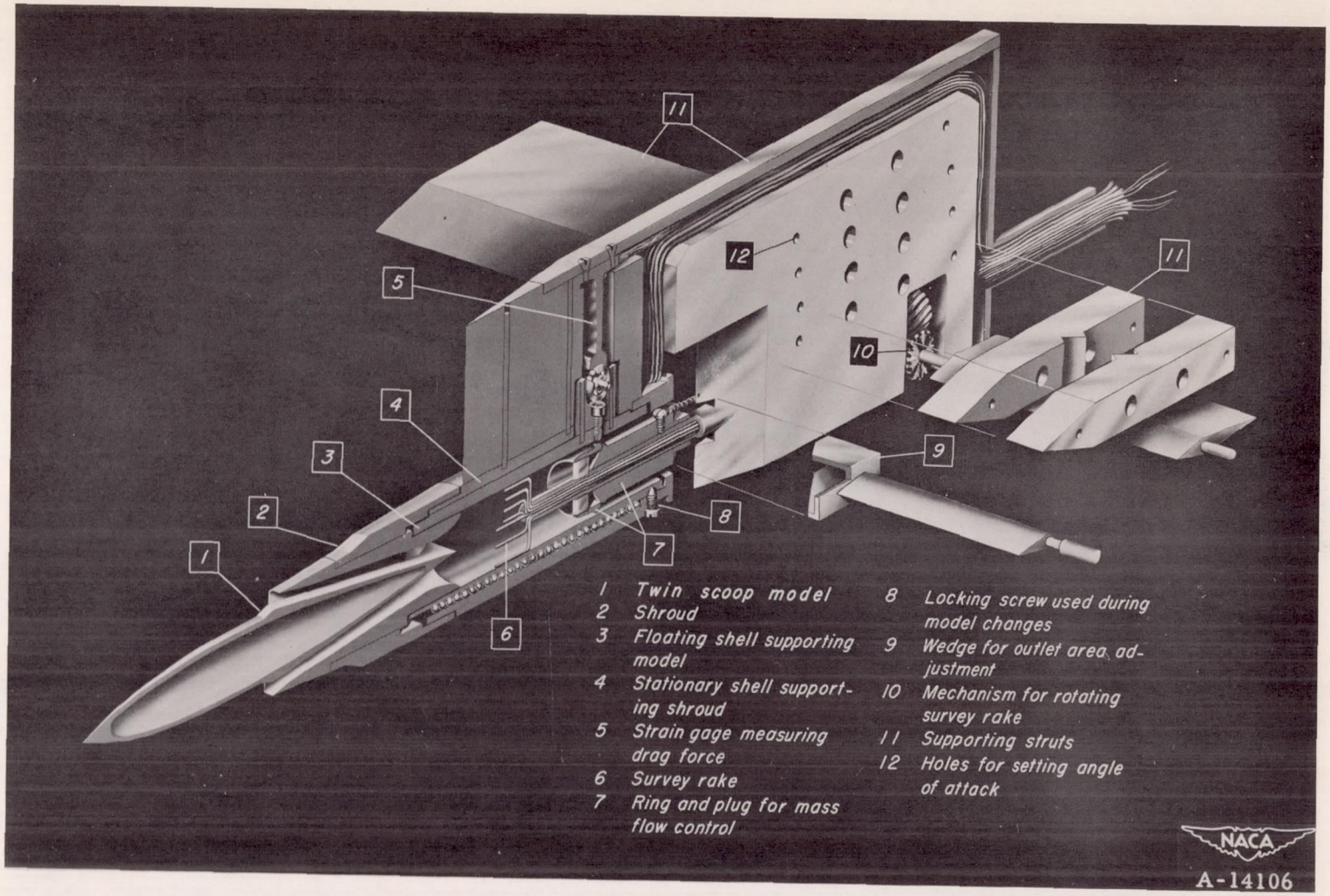

Figure 3.– Apparatus for measuring the performance of supersonic duct inlets.

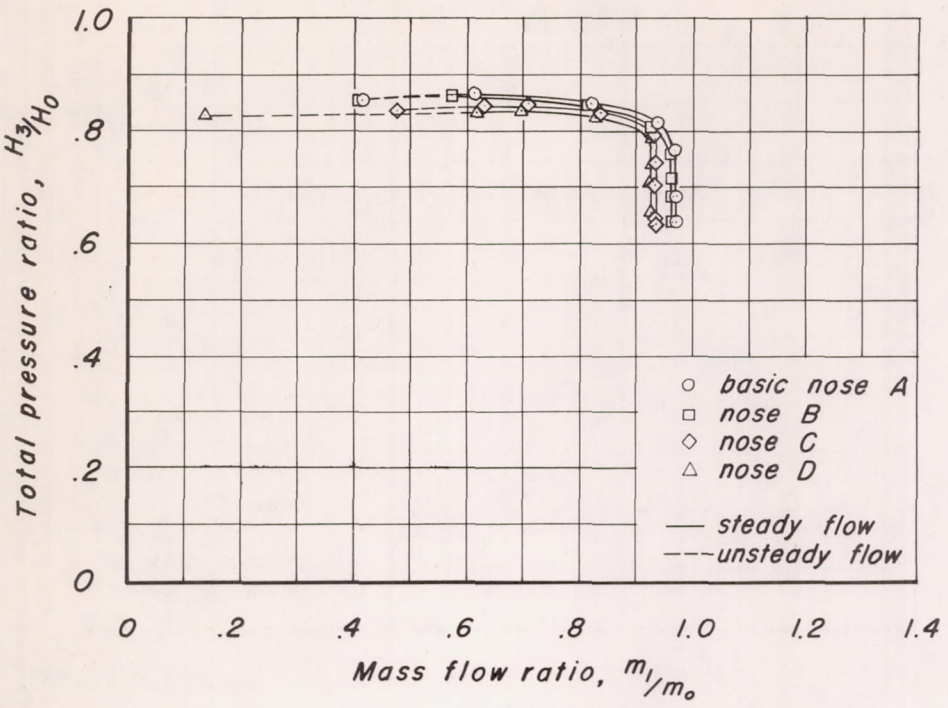

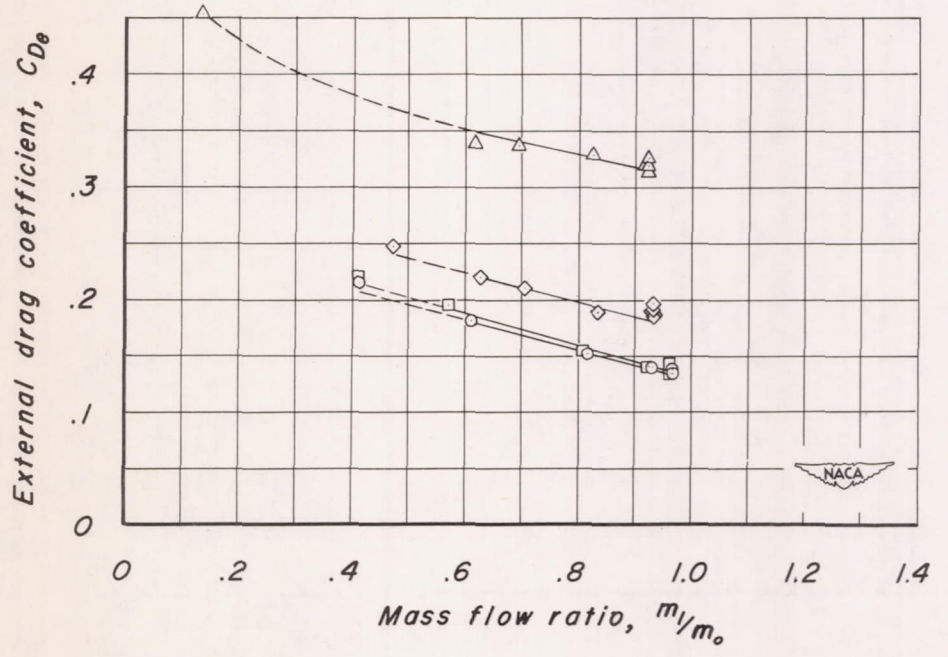

(a) $M_0 = 1.4$, $\alpha = 0°$

Figure 4.- Variation of total-pressure recovery and external drag coefficient with mass-flow ratio for four nose configurations.

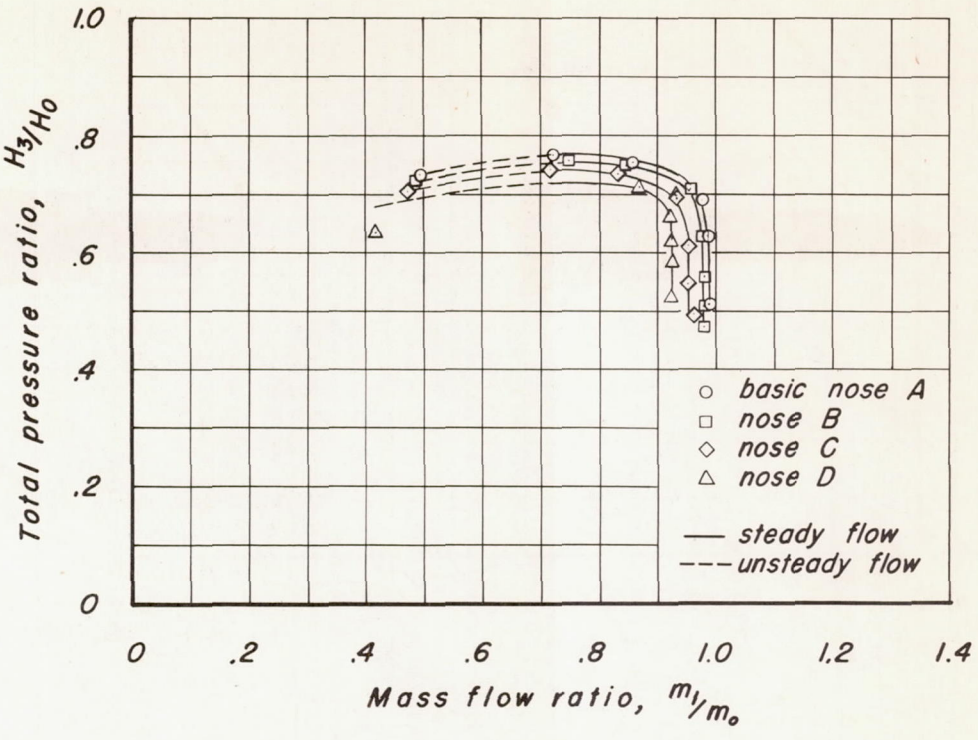

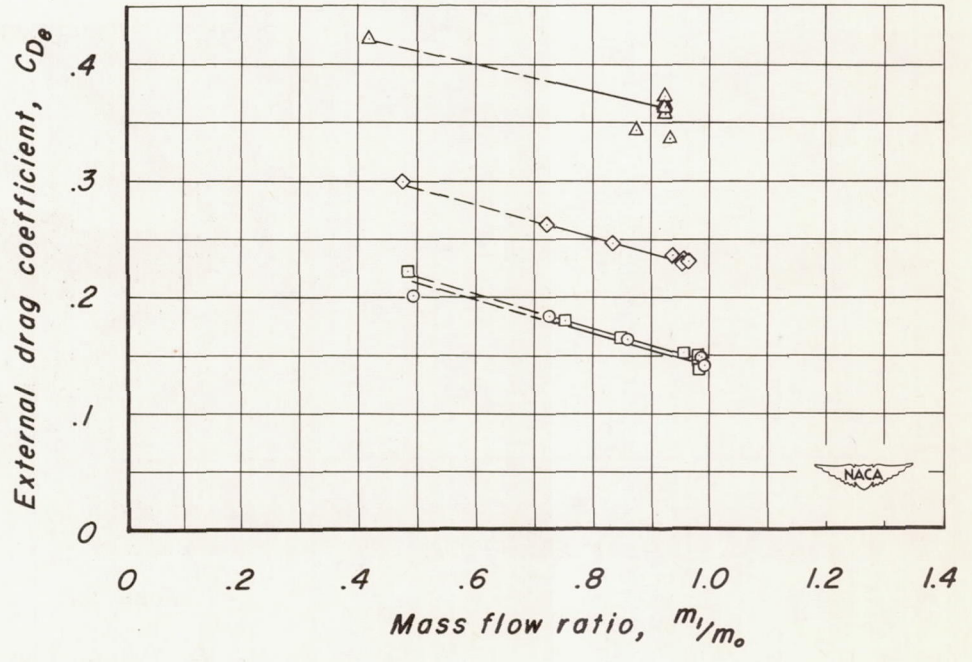

(b) $M_0 = 1.7$, $\alpha = 0°$

Figure 4. - Concluded.

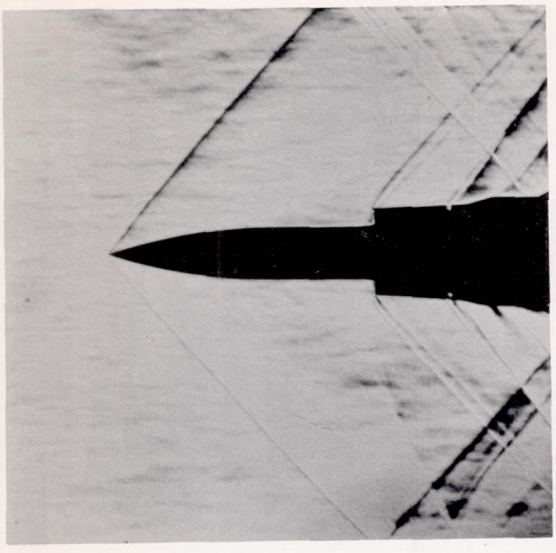

Nose A

$(m_1/m_o)_{max}$=0.970

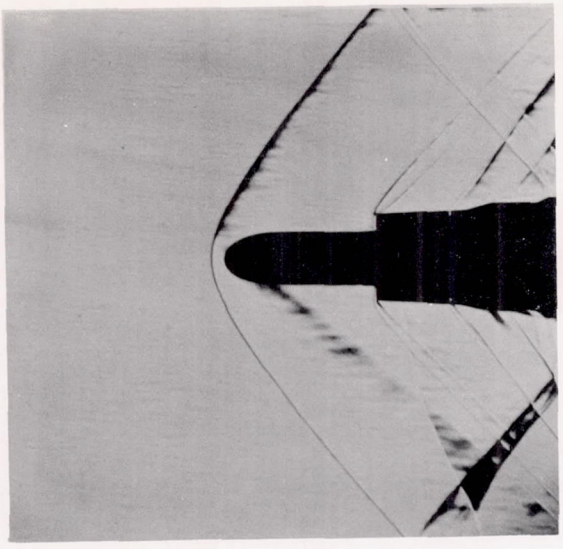

Nose D

$(m_1/m_o)_{max}$=0.925

(a) M_o=1.4

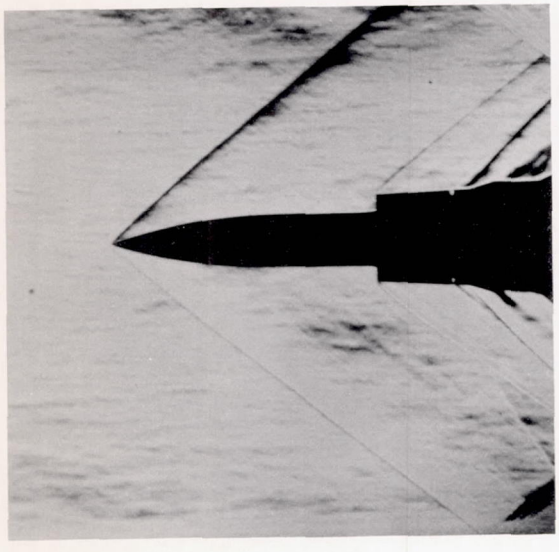

Nose A

$(m_1/m_o)_{max}$=0.990

Nose D

$(m_1/m_o)_{max}$=0.925

(b) M_o=1.7

Figure 5.- Schlieren photographs of model with noses A and D.